ARCHIVES OF BIOCHEMISTRY AND BIOPHYSICS
Vol. 310, No. 2, May 1, pp. 460–466, 1994

X-Ray Structure of the Cytochrome c_2 Isolated from *Paracoccus denitrificans* Refined to 1.7-Å Resolution[1]

Matthew M. Benning,* Terrance E. Meyer,† and Hazel M. Holden*,[2]

*Institute for Enzyme Research, Graduate School and Department of Biochemistry, University of Wisconsin, Madison, Wisconsin 53705; and †Department of Biochemistry, University of Arizona, Tucson, Arizona 85721

Received November 4, 1993, and in revised form January 11, 1994

The cytochrome c_2 (formerly c_{550}) isolated from *Paracoccus denitrificans* is one of the larger bacterial c-type proteins examined thus far. The molecular structure of this cytochrome has been redetermined and refined to 1.7-Å resolution with a crystallographic *R*-factor of 17.5% for all measured X-ray data. Like other, smaller c-type cytochromes, the molecule consists of five α-helices that wrap around the heme group. In addition, this bacterial cytochrome contains two strands of anti-parallel β-sheet, five Type I turns, and three Type II turns. The present model differs from the originally determined structure in several regions including the N-terminus, the loop delineated by Asp 25 to Lys 31, the region defined by Trp 86 to Val 88, and the C-terminus. A total of 103 water molecules has been positioned into the electron density map. Six of these waters are directly involved in heme binding.

The bacterial cytochromes c_2 are a group of proteins typically isolated from photosynthetic nonsulfur purple bacteria where they function as electron carriers in both photosynthesis and respiration (1). These electron transport proteins are characteristically low-spin with the single heme group attached covalently to the protein through thioether linkages between the heme vinyl groups and two cysteine residues located near the N-terminus of the polypeptide chain. The iron of the heme is further ligated to the protein via a histidine and a methionine residue (2). The cytochromes c_2 are the nearest bacterial homologs of mitochondrial c-type cytochromes.

One of the interesting aspects of the bacterial cytochromes c_2 is that, unlike their eukaryotic counterparts, they display far greater variations in both their molecular sizes and oxidation–reduction potentials (2). Consequently, they provide a unique opportunity for investigating those factors, such as hydrogen bonding patterns and solvent structure, thought to modulate the redox potentials and electron transfer rates in cytochrome systems in general. Thus far, the three-dimensional structures of four such cytochromes isolated from *Rhodospirillum rubrum, Paracoccus denitrificans, Rhodobacter capsulatus,* and *Rhodobacter sphaeroides* have been determined to various resolutions (3–7).

We have been studying, by X-ray diffraction techniques, the cytochrome c_2 isolated from *R. capsulatus* since it is one of the larger bacterial cytochromes with 116 amino acid residues and a redox potential of 350 mV (8). In addition, the structural gene for this cytochrome has been cloned (9) and mutant proteins have been expressed and crystallized (10–12). The molecular motif of this protein has been determined and refined to 2.0-Å resolution and, like other c-type cytochromes, its secondary structure consists of five α-helices that surround the heme group (6, 12). As observed in the eukaryotic cytochrome c proteins, but not in the cytochrome c_2 from *R. rubrum,* there are two water molecules buried within the heme binding pocket of the *R. capsulatus* molecule (6).

On the basis of amino acid sequence homology, it was originally suggested that the *R. capsulatus* and the *P. denitrificans* cytochromes were structurally very similar (13). The *P. denitrificans* protein is also one of the larger bacterial c-type cytochromes but unlike the *R. capsulatus* molecule, displays a redox potential of 250 mV which is more similar to the eukaryotic proteins (14). Because of their similarities in structure but differences in biochemical properties, we were interested in comparing in detail these two bacterial cytochromes. The three-dimensional structure of the *P. denitrificans* cytochrome c_2 was solved nearly 18 years ago at a time when X-ray data collection and reduction techniques and molecular graphics software

[1] This research was supported in part by grants from the NIH (GM30982 to H.M.H. and GM21277 to T.E.M.). H.M.H. is an Established Investigator of the American Heart Association.

[2] To whom correspondence should be addressed.

0003-9861/94 $6.00

TABLE I

Intensity Statistics for the Native X-Ray Data Set

		Resolution range							
	Overall	∞-4.08	4.07-3.40	3.39-2.78	2.77-2.40	2.39-2.15	2.14-1.96	1.95-1.82	1.81-1.70
No. of measurements	37,878	1798	5133	6704	7292	6012	3761	3773	3405
No. of independent reflections[a]	12,199	556	1037	1324	1558	1743	1893	2010	2078
		(373)	(929)	(1293)	(1515)	(1399)	(959)	(980)	(920)
% of the Theoretical No. of reflections	97	89	98	100	98	100	97	100	92
Average intensity		2768	3184	1449	820	577	392	199	109
Sigma		103	118	63	47	42	22	16	14
R-factor[b] (%)	3.8	1.9	2.3	2.9	3.9	4.7	4.0	5.9	9.4

[a] This is the number of reduced observations. Shown in parentheses is the number of independent measurements for which there were duplicate or symmetry related observations.

[b] $R\text{-factor} = \Sigma|I - \bar{I}|/\Sigma I \times 100$.

and hardware were less sophisticated (5). Consequently, while the overall fold of the *P. denitrificans* cytochrome c_2 originally determined was correct with some minor ambiguities (15), the model was never refined. Furthermore, the X-ray data was not at high enough resolution to locate accurately the positions of ordered water molecules. Here we describe the structure of the oxidized *P. denitrificans* cytochrome c_2 redetermined and refined to 1.7-Å resolution. X-ray coordinates for this cytochrome have been deposited in the Brookhaven Protein Data Bank (16) or may be obtained immediately via holden@enzyme.wisc.edu.

MATERIALS AND METHODS

Crystallization. The oxidized cytochrome c_2 used in this investigation was isolated and purified as previously described (15, 17). Large, single crystals were grown at room temperature by the hanging drop method of vapor diffusion against 3.3 to 3.5 M ammonium sulfate solutions buffered with 50 mM Hepes[3] at pH 7.5. The crystals obtained were the same as previously employed for the original structure determination of the *P. denitrificans* cytochrome c_2 (18) and belonged to the space group $P2_12_12_1$ with unit cell dimensions of a = 31.6 Å, b = 42.1 Å, c = 81.6 Å and one molecule per asymmetric unit.

X-ray data collection and reduction. X-ray data to 1.7-Å resolution were collected from a single crystal at 4°C with a Siemens X1000D area detector system. The X-ray source was nickel-filtered copper Kα radiation from a Rigaku RU200 X-ray generator operated at 50 kV and 50 mA. The X-ray data were processed with the software package XDS (19) and internally scaled according to the algorithm of Fox and Holmes as implemented by Dr. Phil Evans (20). Of the 37,878 intensity measurements recorded, 12,199 were unique reflections. The X-ray data set contained 97% of the total theoretical number of observations to 1.7-Å resolution. Relevant X-ray data collection statistics may be found in Table I.

Computational methods. With the previously determined structure of the *P. denitrificans* cytochrome c_2 serving as a starting model (5), an initial cycle of refinement was conducted by the method of simulated

[3] Abbreviation used: Hepes, 4-(2-hydroxyethyl)-1-piperazineethanesulfonic acid.

TABLE II

Refinement Statistics

Resolution limits (Å)	30.0-1.7
R-factor (%)[a]	17.5
No. of reflections used	12,199
No. of protein atoms	960
No. of solvent molecules	103
Weighted root-mean-square deviations from ideality	
Bond length (Å)	0.007
Bond angle (degrees)	2.264
Planarity (trigonal) (Å)	0.003
Planarity (other planes) (Å)	0.008
Torsion angle (degrees)[b]	16.35

[a] $R\text{-factor} = \Sigma|F_O - F_C|/\Sigma|F_O|$.

[b] The torsion angles were not restrained during the refinement.

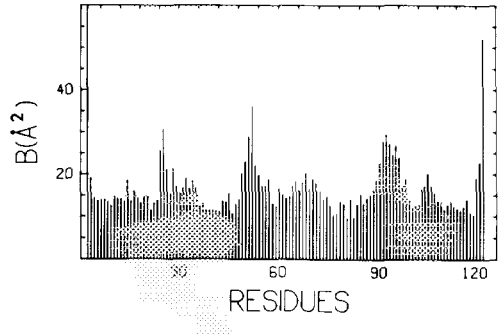

FIG. 1. Plot of the mean *B*-value versus amino acid residue for all main-chain atoms. Only the backbone atoms for amino acid residue 2 have large *B*-values. Excluding this residue, the average temperature factor for the backbone atoms is 16.2 Å².

TABLE III

List of Secondary Structural Elements

Residue No.	Type of structure
Ala 5–Cys 15	α-Helix
Lys 16–His 19	Reverse turn
Met 20–Gln 22	β-sheet
Ala 23–Gly 26	Reverse turn
Thr 27–Ile 30	β-sheet
Leu 39–Val 42	Reverse turn
Val 42–Arg 45	Reverse turn
Glu 50–Phe 53	Reverse turn
Glu 57–Lys 65	α-Helix
Asn 66–Leu 69	Reverse turn
Glu 73–Thr 81	α-Helix
Pro 83–Thr 91	α-Helix
Asp 93–Ala 96	Reverse turn
Gln 108–Gln 117	α-Helix
Ser 119–Ala 122	Reverse turn

annealing as implemented in the software package, X-PLOR (21). Following this initial stage of refinement, an electron density map was calculated with X-ray data from 30- to 2.5-Å resolution and coefficients of the form $(2F_o - F_c)$. From this map it was possible to correct the amino acid sequence errors found in the original three-dimensional model of the protein (15). Additional cycles of restrained least-squares refinement and manual model building with the software packages, TNT and FRODO, respectively, reduced the R-factor to 17.5% for all measured X-ray data from 30.0 to 1.7 Å (22, 23). "Ideal" stereochemistry for the heme group was based on the small molecule structure determination of Anderson *et al.* (24). Relevant refinement statistics are listed in Table II. Peaks of electron density were considered to be water molecules if they were located within 4.0 Å of potential hydrogen-bonding groups. There were 103 water molecules positioned into the electron density map. The average B-value for these water molecules was 36.8 Å^2 with 34 having B-values below 30.0 Å^2. A plot of the mean main chain temperature factors may be found in Fig. 1 and a Ramachandran diagram of all nonglycinyl residues is depicted in Fig. 2. There were seven amino acid residues with dihedral angles lying slightly outside of the theoretically allowed regions (Cys 18, Ala 48, Lys 84, Thr 91, Asp 92, Ala 96, and Asn 107).

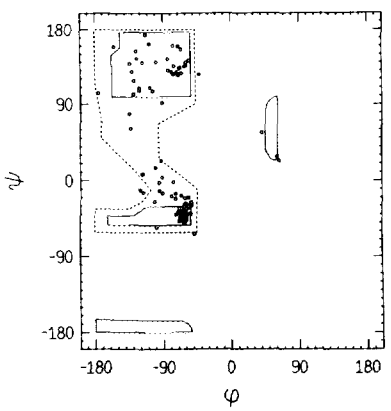

FIG. 2. A Ramachandran plot of all nonglycinyl main chain dihedral angles.

TABLE IV

Dihedral Angles for Reverse Turns

Amino acid residue No.	Type of turn	ϕ_2	ψ_2	ϕ_3	ψ_3
Lys 16–His 19	~I	−61.1	−29.3	−119.5	−12.7
Ala 23–Gly 26	I	−55.1	−29.0	−77.3	−1.9
Leu 39–Val 42	~II	−62.3	136.1	61.7	25.3
Val 42–Arg 45	II	−71.1	125.6	90.7	−7.4
Glu 50–Phe 53	II	−68.2	133.2	77.9	−8.3
Asn 66–Leu 69	I	−59.1	−28.6	−91.1	3.1
Asp 93–Ala 96	I	−53.8	−29.7	−95.6	8.3
Ser 119–Ala 122	I	−55.9	−30.8	−100.5	14.4

RESULTS AND DISCUSSION

Representative portions of the electron density map for the redetermined structure are shown in Fig. 3. For

TABLE V

Differences in Dihedral Angles

	Refined X-ray coordinates		Original X-ray coordinates	
Residue No.	ϕ	ψ	ϕ	ψ
Asp 4	−108.2	109.3	−92.7	−135.4
Ala 5	−60.3	−28.0	174.4	−42.3
Ile 21	−129.6	101.3	−124.4	−64.7
Gln 22	−130.2	128.2	35.4	173.6
Ala 23	−65.2	156.0	−136.5	−177.8
Tyr 40	−62.3	136.1	−75.6	148.3
Gly 41	61.6	25.4	90.1	−75.0
Val 42	−66.6	−34.5	16.9	−99.7
Arg 45	−83.6	144.9	−27.7	−101.6
Lys 46	−60.7	139.5	147.2	100.6
Ser 49	−116.8	6.8	−50.4	−91.6
Glu 50	−66.2	127.0	6.2	113.6
Asp 68	−91.2	3.2	−68.5	−71.7
Leu 69	−75.8	124.8	−20.8	88.7
Trp 71	−71.2	127.1	0.8	73.8
Thr 72	−107.6	161.4	−42.3	−114.8
Glu 73	−59.3	−41.4	−174.9	8.3
Leu 87	−62.9	−41.4	−65.8	150.7
Val 88	−61.1	−43.7	87.5	−150.4
Lys 89	−58.2	−50.6	32.8	−72.5
Asp 92	62.5	27.1	100.3	−18.4
Asp 93	−120.8	108.8	−71.1	109.3
Lys 94	−53.8	−29.7	−75.2	137.9
Gly 95	−95.6	8.2	106.3	52.3
Ala 96	−43.0	123.6	−48.2	−96.5
Lys 97	−96.2	140.4	136.8	−63.4
Thr 98	−117.7	140.1	57.8	169.4
Lys 106	−153.7	158.8	−111.9	−40.6
Asn 107	64.6	22.5	−131.4	61.2
Asn 118	−93.7	23.4	−59.3	−33.2
Ser 119	−133.7	60.8	−98.1	83.5
Asp 121	−100.5	14.4	−87.6	119.7

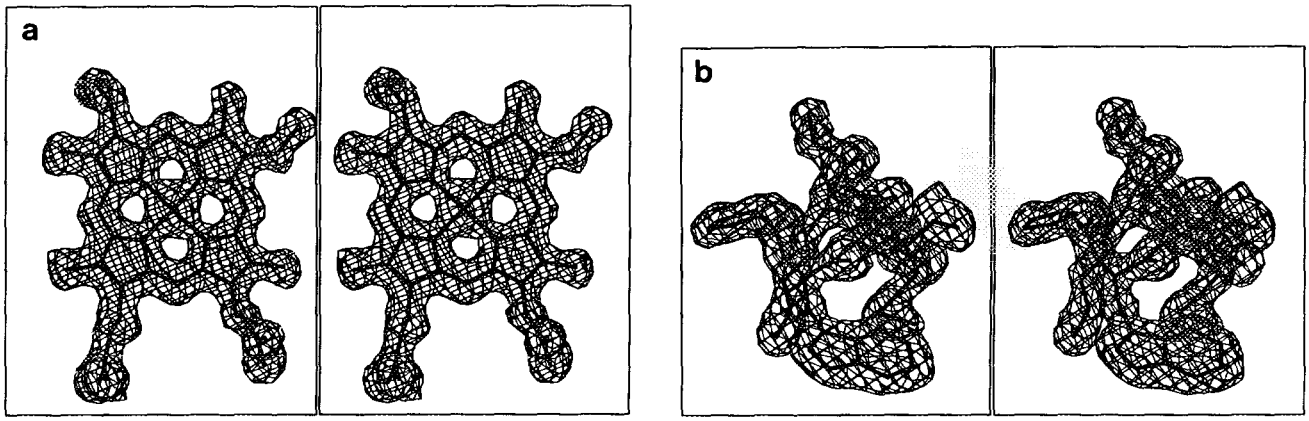

FIG. 3. Representative sections of the electron density map calculated to 1.7-Å resolution. The electron density shown was calculated with coefficients of the form ($2Fo - Fc$) and contoured at 1σ. (a) Electron density associated with the heme group. (b) Electron density corresponding to residues Pro 85, Trp 86, Leu 87, Val 88, Lys 89, and Met 90. Trp 86 was thought to be a leucine residue in the original *P. denitrificans* structure.

the most part, the electron density was well-ordered except for the lysine residues. Of the 16 lysine residues in the protein, the side chain densities for 11 were disordered (amino acid residues 7, 10, 16, 31, 34, 54, 65, 94, 97, 103, and 106). With respect to the ordered lysine residues, Lys 14 and Lys 89 were involved in crystalline contacts, Lys 84 and Lys 99 formed electrostatic interactions with the carbonyl groups of Ala 96 and Lys 54, respectively, and the amino terminal group of Lys 46 was anchored in place by three water molecules. In addition to the lysine residues, the side chain electron densities for Asp 2, Glu 51, Glu 57, and Glu 64 were weak and there was no electron density for the N-terminal glutamine residue. Amino acid sequence analyses suggest that this larger bacterial cytochrome c contains 128 residues although the gene sequence shows 135 amino acid residues in the native protein (15, 25). In the structural analysis described here, there was no electron density beyond Ala 122 in electron density maps contoured at 1σ and calculated with coefficients of the form ($2F_o - F_c$). It is possible that some endogenous proteolysis may have occurred at the C-terminus during protein purification. The isocytochrome c_2 isolated from *R. sphaeroides* also has an extended C-terminus which may be subject to post-translational proteolysis (26).

The secondary structural elements found in this cytochrome are listed in Table III and a ribbon representation of the molecule is displayed in Fig. 4. Like the cytochrome isolated from *R. capsulatus*, the *P. denitrificans* protein contains five α-helices and two strands of anti-parallel β-pleated sheet (6). The protein also contains five Type I turns and three Type II turns. Dihedral angles for these reverse turns are given in Table IV.

A superposition of the original protein model and that determined in this investigation is shown in Fig. 5. The α-carbons for these two models superimpose with a root-mean-square deviation of 1.1 Å. Those dihedral angles that differ significantly between the two structures are listed in Table V. The most striking differences in the two structures reside in the surface loop delineated by Asp 25 to Lys 31 as can be seen in the superposition displayed in Fig. 6. In the refined model presented here, there is an extra isoleucine residue inserted between Ile 29 and Lys 31. In addition to this loop region, the other major differences in the two models occur at amino acid residues 86 and 88. These residues, built into the original structure as Leu 86 and Lys 88, are clearly Trp 86 and Val 88 as suggested by Ambler *et al.* (15). Val 88 is located toward the surface of the molecule while $N^{\epsilon 1}$ of Trp 86 hydrogen bonds to a water molecule (2.77 Å). The plane of the side chain for Trp 86 lies roughly parallel, but displaced, to that of Trp 71, which is located in the heme binding

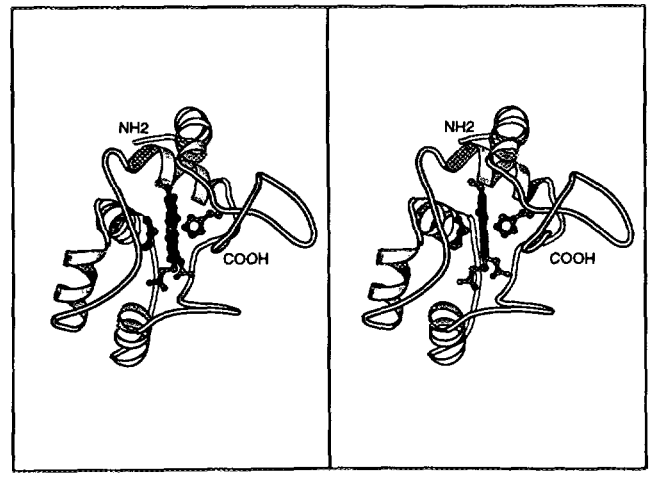

FIG. 4. Ribbon representation of the *P. denitrificans* cytochrome c_2. This figure was prepared with the program MOLSCRIPT (27).

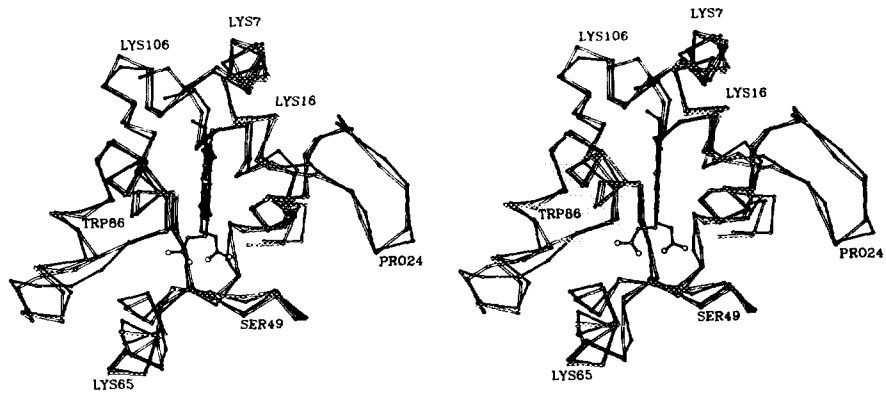

FIG. 5. Superposition of the α-carbons for the original *P. denitrificans* structure and the refined model. The original and refined models are displayed in open and solid bonds, respectively.

pocket. These two aromatic residues participate in stacking interactions with the closest approach of atoms in their side chains being 3.71 Å.

A close-up view of the heme binding pocket is given in Fig. 7. There are five aromatic residues near the heme, namely Phe 53, Tyr 55, Trp 71, Tyr 79, and Phe 102 and six well-ordered water molecules. Met 100 and His 19 serve as the heme ligands with the S^{δ} and $N^{\epsilon 2}$ of these residues being 2.35 and 1.93 Å, respectively from Fe^{+3}. The hydrogen bonding pattern around the heme propionates in the *P. denitrificans* cytochrome c_2 is very similar to that observed in the *R. capsulatus* protein with respect to both bond lengths and geometrical constraints (6). Specifically, the carboxyl oxygen, $O^{1\alpha}$, of the buried propionate is within hydrogen bonding distance of O^{η} of Tyr 55 (2.61 Å) and $N^{\eta 2}$ of Arg 45 (2.96 Å) while the other carboxyl oxygen of the propionate, $O^{2\alpha}$, participates in hydrogen bonding interactions with $N^{\epsilon 1}$ of Trp 71 (2.83 Å) and the backbone nitrogen of Ala 48 (3.02 Å). Both of these carboxyl oxygens lie within 2.78 and 3.16 Å, respectively, of a well-ordered water molecule. Likewise, as in the *R. capsulatus* cytochrome, the more exposed heme propionate side chain participates in hydrogen bonds with backbone amide hydrogens and two water molecules. The carboxyl oxygen of the heme propionate, $O^{1\delta}$, interacts with the backbone amide group of Gly 56 (2.64 Å), whereas the carboxylate oxygen, $O^{2\delta}$, lies within hydrogen bonding distance of the backbone nitrogen of Lys 99 (2.95 Å) and two water molecules (2.85 and 2.79 Å). Two of the other water molecules located in the heme binding pocket participate in hydrogen bonds to backbone atoms. Specifically, one serves to bridge the amide nitrogens of Thr 101 and Phe 102 and the other links the carbonyl oxygens of Val 80 and Phe 102. The sixth water molecule within the vicinity of the heme prosthetic group lies at 3.38 Å from O^{γ} of Thr 35.

There are 103 ordered water molecules modeled into the electron density map with most being located at the surface of the protein. Ten of these waters serve to bridge directly neighboring cytochrome molecules within the crystalline lattice. Twelve of the water molecules have temperature factors below 20 $Å^2$, five of which are located in the heme binding pocket as described above and shown in Fig. 7. Of the remaining seven with very low temperature factors, four are located at the protein surface, one serves to stabilize the loop preceding the conserved Pro 37 by hydrogen bonding to the carbonyl oxygens of Gly 33 and Gly 36, one bridges the carbonyl oxygens of Asn 66 and Leu 69 to N^{ζ} of Lys 46, and finally, the most ordered water molecule, with a temperature factor of 10.6 $Å^2$, resides at the end of the fourth helix where it interacts with the carbonyl oxygens of Glu 78 and Asp 82.

When the *P. denitrificans* and the *R. capsulatus* cytochrome c_2 structures are superimposed, 11 of the 103 water molecules adopt positions within 1.0 Å of each other in

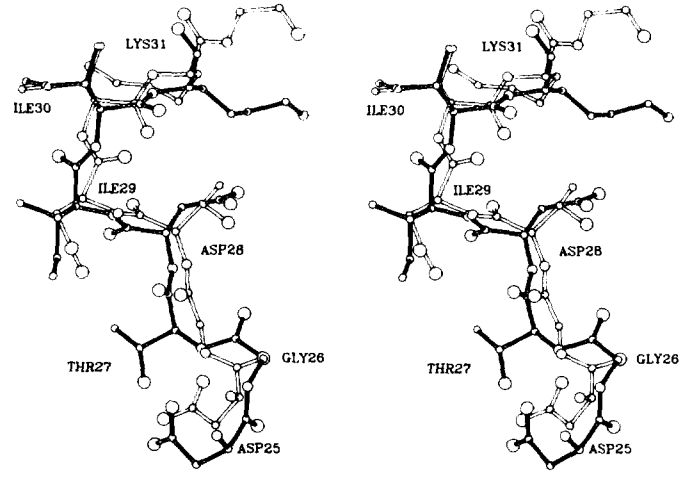

FIG. 6. Superposition of the loop delineated by Asp 25 to Lys 31 in the original and refined cytochrome structures. The original model is shown in open bonds while the refined model is displayed in a solid representation.

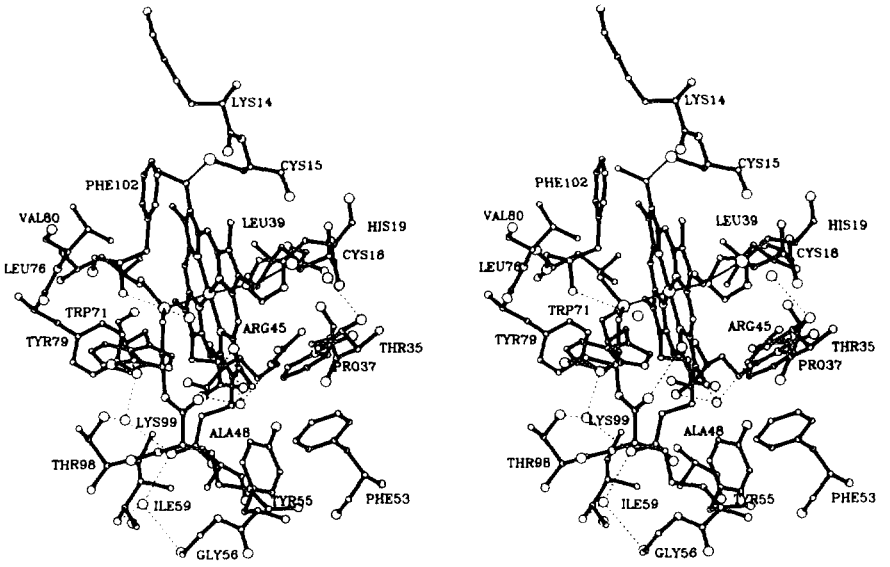

FIG. 7. Close-up view of the heme binding pocket. Only those amino acid residues that are within approximately 4.0 Å of atoms of the heme are shown. Water molecules are displayed as circles. The dashed lines represent putative hydrogen bonding interactions between these waters and the protein.

the two proteins as shown in Fig. 8. Like that observed in the *P. denitrificans* protein, the water molecule stabilizing the loop preceding the conserved proline is found in the *R. capsulatus* cytochrome. Also, three of these waters are located in the heme binding region. The remaining structurally "conserved" waters between these two bacterial cytochromes are found at the surface. However, they are not randomly distributed throughout the molecular surface but rather are located on the right side of the heme binding crevice as can be seen in Fig. 8. Whether the clustering of these waters at one surface of the protein is merely fortuitous or is important in the biological function of these bacterial cytochromes is presently unknown.

The overall fold of the *P. denitrificans* cytochrome c_2, as originally determined, was basically correct although details concerning hydrogen bonding patterns and solvent structure were missing due to limitations in both hardware and software. With the recent advances in protein crystallography made during the past decade, however, it is timely and worthwhile in many cases to recollect X-ray data and to refine initial protein models by least-squares procedures so that as much biochemical information as possible may be obtained from a crystal structure. Clearly, well-determined and refined models are essential for understanding the structural nuances often associated with site-directed mutants of a respective protein. Now that the *P. denitrificans* cytochrome model has been refined, it will be possible to conduct detailed comparisons of it with other bacterial c-type cytochromes in an effort to understand on a three-dimensional level those factors that

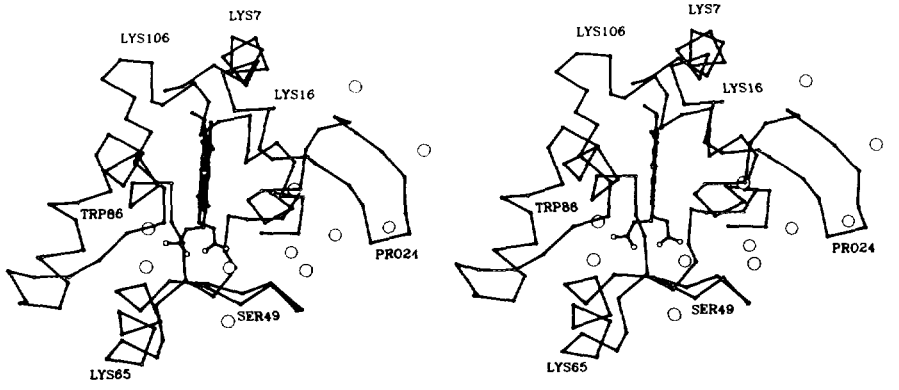

FIG. 8. Position of the conserved water molecules between the *P. denitrificans* and the *R. capsulatus* cytochromes c_2. The α-carbon trace shown is that of the *P. denitrificans* protein with the conserved waters displayed as large circles.

modulate oxidation–reduction potentials and electron transfer rates within this family of proteins. These comparisons, along with site-directed mutagenesis experiments with the *R. capsulatus* cytochrome c_2, are presently in progress.

REFERENCES

1. Bartsch, R. G. (1978) Cytochromes. *in* The Photosynthetic Bacteria (Clayton, R. K., and Sistrom, W. R., Eds.), pp. 249–279, Plenum, New York.
2. Meyer, T. E., and Kamen, M. D. (1982) New perspectives on *c*-type cytochromes. *in* Advances in Protein Chemistry (Anfinsen, C. B., Edsall, J. T., and Richards, F. M., Eds.), Vol. 35, pp. 105–212, Academic Press, New York.
3. Salemme, F. R., Freer, S. T., Xuong, Ng, H., Alden, R. A., and Kraut, J. (1973) *J. Biol. Chem.* **248,** 3910–3921.
4. Bhatia, G. E. (1981) Ph.D. thesis, pp. 1–122, University of California, San Diego.
5. Timkovich, R., and Dickerson, R. E. (1976) *J. Biol. Chem.* **251,** 4033–4046.
6. Benning, M. M., Wesenberg, G., Caffrey, M. S., Bartsch, R. G., Meyer, T. E., Cusanovich, M. A., Rayment, I., and Holden, H. M. (1991) *J. Mol. Biol.* **220,** 673–685.
7. Axelrod, H. L., Feher, G., Allen, J. P., Day, M., Chirino, A., Hsu, B. T., and Rees, D. C. (1992) Biophysical Society Meeting, Houston TX, 1992, Poster 596a.
8. Tollin, G., Cheddar, G., Watkins, J. A., Meyer, T. E., and Cusanovich, M. A. (1984) *Biochemistry* **23,** 6345–6349.
9. Daldal, F., Cheng, S., Applebaum, J., Davidson, E., and Prince, R. C. (1986) *Proc. Natl. Acad. Sci. USA* **83,** 2012–2106.
10. Caffrey, M. S. (1991) Ph.D. thesis, University of Arizona, Tucson, AZ.
11. Caffrey, M., Davidson, E., Cusanovich, M., and Daldal, F. (1992) *Arch. Biochem. Biophys.* **292,** 419–426.
12. Benning, M. M., Fitch, J., Meyer, T. E., Cusanovich, M. A., and Holden, H. M., unpublished results.
13. Timkovich, R., Dickerson, R. E., and Margoliash, E. (1976) *J. Biol. Chem.* **251,** 2197–2206.
14. Meyer, T. E., Przysiecki, C. T., Watkins, J. A., Bhattacharyya, A., Simondsen, R. P., Cusanovich, M. A., and Tollin, G. (1983) *Proc. Natl. Acad. Sci. USA* **80,** 6740–6744.
15. Ambler, R. P., Meyer, T. E., Kamen, M. D., Schichman, S. A., and Sawyer, L. (1981) *J. Mol. Biol.* **147,** 351–356.
16. Bernstein, F. C., Koetzle, T. F., Williams, G. J. B., Meyer, E. F. Jr., Brice, M. D., Rogers, J. R., Kennard, O., Shimanouchi, T., and Tasumi, M. (1977) *J. Mol. Biol.* **112,** 535–542.
17. Scholes, P. B., McLain, G., and Smith, L. (1971) *Biochemistry* **10,** 2072–2076.
18. Timkovich, R., and Dickerson, R. E. (1973) *J. Mol. Biol.* **79,** 39–56.
19. Kabsch, W. (1988) *J. Appl. Crystallogr.* **21,** 67–71.
20. Fox, G. C., and Holmes, K. C. (1966) *Acta Crystallogr.* **20,** 886–891.
21. Brunger, A. T. (1990) X-PLOR Manual, Version 2.1, Yale University, New Haven, CT.
22. Tronrud, D. E., Ten Eyck, L. F., and Matthews, B. W. (1987) *Acta Crystallogr.* **43**(A), 489–501.
23. Jones, T. A. (1985) *Methods Enzymol.* **115,** 157–171.
24. Anderson, O. P., Schauer, C. K., and Caughey, W. S. (1982) *Am. Crystallogr. Assoc.* **10**(2), 23.
25. Van Spanning, R. J. M., Wansell, C., Harms, N., Oltmann, L. F., and Stouthamer, A. H. (1990) *J. Bacteriol.* **172,** 986–996.
26. Rott, M. A., Witthuhn, V. C., Schilke, B. A., Soranno, M., Ali, A., and Donohue, T. J. (1993) *J. Bacteriol.* **175,** 358–366.
27. Kraulis, P. J. (1991) *J. Appl. Crystallogr.* **24,** 946–950.